Title

A Bayesian recursive framework for ball-bearing damage classification in rotating machinery

Journal

Structural Health Monitoring, 15(6)

ISSN

1475-9217

Authors

Mao, Zhu

Todd, Michael D

Publication Date

2016-11-01

DOI

10.1177/1475921716656123

Peer reviewed

A Bayesian Recursive Framework for Ball Bearing Damage Classification in Rotating Machinery

Zhu Mao[1,2] and **Michael Todd**[2*]

[1] Department of Mechanical Engineering, University of Massachusetts Lowell
1 University Avenue, Lowell, MA, USA 01854-5104
[2] Department of Structural Engineering, University of California, San Diego
9500 Gilman Drive, MC0085, La Jolla, CA, USA 92093-0085

Abstract

Extracting damage-sensitive features plays an important role in all structural health monitoring (SHM) applications, as it determines the metrics on which to base decision-making with regard to operation, maintenance, damage state, etc. This paper adopts the widely-employed frequency response function (FRF), both its magnitude and phase, as the selected feature source, and demonstrates how the damage types and locations are able to be classified by means of Bayesian recursive confidence updating. The features are estimated from the in-situ acquired vibration data on a rotating machinery test-bed, and the probabilistic models that quantify feature uncertainty are the likelihood functions in a Bayesian framework, which informs the most plausible decisions based on the collected evidence. The damage classification effort in this paper specifically calculates the posterior probability, considering the prior and likelihood of data observations; posterior probabilities are then fed back as prior probabilities in the next iteration as new test data are observed. There are three ball-bearing damage conditions applied to the rotary machine test-bed, and the correct model representing the correct damage types will be selected by the model with the maximum posterior confidence. Classification via posterior probability is shown in this paper to outperform traditional

*Corresponding author
Phone: +1-858-534-5951
Email: mdtodd@ucsd.edu

likelihood evaluations, and the Bayesian recursive implementation distinguishes all three conditions in this work.

Keywords: Damage Classification, Rotating Machinery, Structural Health Monitoring, Condition-Based Monitoring, Ball Bearing, Bayes' Theorem

1. Introduction

As the operating life cycles of all sorts of machinery and infrastructure systems get more demanding, both offline nondestructive evaluation (NDE) and in-situ structural health monitoring (SHM) play an increasingly important role in overall life cycle management. This NDE/SHM paradigm aims to provide state awareness by detecting, localizing, and classifying damage, as well as to forecast the trend in the damage progression. In a lot of occasions, NDE is conducted in an offline fashion after precursors to damage have been flagged from online SHM systems [1]. The origin of the four-step SHM process may trace back to Rytter's doctoral thesis where the aforementioned four levels are described as [2]:

- Existence: detection of the presence of the defects that could affect the system functionality
- Location: determination of the damage position
- Extent: identification of the damage details, such as type(s) and severity
- Prediction: prognosis of the structural defects

The application of this process aims to enable system owners to convert from the traditional event- and/or time-based maintenance scheduling to condition-based scheduling. Another partition is often adopted in terms of pre- and post-event analysis, namely, diagnosis and prognosis, in which the former deals with the first three

levels, and the latter concerns the fourth level prior-event analysis [3]. In the context of SHM, the damage to be identified is defined as "changes introduced into a system that adversely affect its current or future performance [4]." Despite this performance-based concept of damage, there are other related terminologies with subtly different meanings. Worden et al. deliberate the difference and conclude with a hierarchical relationship between different notations [1]: *fault* is when the system is not operating satisfactorily as it is designed to; *damage* is when the operation is not ideal but is still functioning satisfactorily in a suboptimal manner; and *defect* means unknown inherent imperfections that might cause problems in the future. Other than the abovementioned SHM-related concepts, condition monitoring (CM) and Condition-Based Maintenance (CBM) often exist in the literature as well, and may refer to the relevant activities but have slightly different emphases. CM is mostly used in the field of rotating and manufacturing machineries, and the CM data cover a very broad range beyond just structural health assessment [1] [3]. CBM, which literally emphasizes maintenance scheduling, is essentially the same idea as SHM, and is interpreted as the flow of data acquisition, processing, and post decision-making, targeting the capability of damage diagnosis and prognosis. A thorough survey on CBM and SHM endeavors is available in Ref. 3 and 5.

Among all the interpretations of the four-level SHM, the most well-accepted description is given by Farrar et al., which addresses the process as a statistical pattern recognition paradigm, and the entire flow is partitioned into four steps: operational evaluation, data acquisition and cleansing, feature extraction, and statistical model development [6]. Inspired by the data-based framework and statistical pattern recognition idea, a large body of research has been deployed in interpreting SHM signals assisted with physics-based system modeling [5], and this paper will later on classify bearing damages with respect to statistics-rooted classification by means of Bayesian model selection.

From a more general perspective, a great number of SHM components are essentially discretizing continuous problems into a finite number of states, and decisions are made among those pre-defined choices. For instance, damage detection is the process of discriminating the damaged system from undamaged state, which is a binary labeling. Damage localization may be regarded as the selection among finite candidate positions in the spatial domain. Specifically to the scope of this paper, classifying the type of damage is thereby a finite-state mapping, in which all possible damaged conditions are grouped into a discretized damage space. Among the four levels of SHM, the first two levels (detection and localization) may only consider information from undamaged state (an unsupervised learning scenario). For the classification on the third level, according to the SHM axioms, the algorithms have to involve information from other candidate states as a supervised learning process, and the information is acquired from either testing measurements or physical modeling [5,7]. Apparently, classification of different types of damages falls into the scenario of supervised learning implementation, and knowledge of each candidate damaged condition should be available before deploying the proposed framework in this paper. A substantial body of work over the past couple of decades has been targeted to identify the types and locations of potential defects and/or damages, by means of modeling and analyzing the in-situ acquired time series in the time domain [8–11], or in the time-frequency domain [12–15]. Moreover, as the complexity of SHM implementations getting higher, modern data-acquisition and processing methodologies are also widely adopted in CBM and SHM for damage diagnosis and classification, such as compressive sensing, Markov chain, Bayesian inference, etc., as reported in Refs. 16–24.

In this specific paper, damage classification of rotating machinery will be the focus, which forms a subcategory of the abovementioned general damage identification activities. There are numerous forms of rotating machinery widely spanning the mechanical and aerospace engineering domains, such as power generators/transmissions, vehicle engines, turbines, propellers, compressors/pumps, gyroscopes, and so on.

The most common components of rotary machines being monitored are bearings and gears, whose SHM features are often interpretable physically, and the aforementioned general algorithms have been employed to enhance their reliability and maintenance quality. As a very well-developed technique, the four characteristic fault frequencies are able to differentiate most of the monitored conditions and may be utilized to localize the fault location, namely, inner race, outer race, ball, or cage. Those fundamental frequencies include the Ball Pass Frequency of Inner Race (BPFI), Ball Pass Frequency of Outer Race (BPFO), Fundamental Train Frequency (FTF) and Ball Spin Frequency (BSF) respectively, and are determined by bearing geometry and operating speed [25]. The damage classification via four characteristic fault frequencies is based on the change of rattling pattern, extracted from the power spectra of vibrational data, when different damage cases occurred. Other traditional detector and classifiers for bearing and gearbox damages are also widely adopted, such as vibration statistics and frequency response analysis. Kurtosis (fourth order statistical moment) is employed as a method for rolling element bearing damage identification [26], and point-defects of bearings on inner/outer race, or general roughness changes are classified facilitated by frequency response analysis [27]. In addition to extracting the straightforward features, the abovementioned state-of-the-art diagnosis methodologies for general applications are also applied in the rotary machine SHM implementations. For instance, Wigner-Ville distribution is adopted in gearbox condition monitoring and based on statistical and neural pattern recognition, local tooth faults of spur gears may be detected [28]. Wavelet-based methodologies for rotating machine damage diagnosis are reviewed in Ref. 29, and the theory and applications of wavelets are summarized, as well as the new research trends, such as wavelet finite element, dual-tree complex wavelet transform, wavelet function design and selection. Empirical mode decomposition (EMD) and autoregressive (AR) model are adopted for more complicated feature extraction of operating ball bearings. The former one decomposes the non-stationary vibration data into a series of intrinsic mode function (IMF) components, and AR coefficients and

the residual variance of the AR models are selected as damage indexes. By means of the data-driven process, the patterns of different types of damages are studied for damage classification [30]. Facilitated by the machine learning technologies, Relevance Vector Machine (RVM) and Support Vector Machine (SVM) are adopted to process rotary machine condition monitoring data [31, 32], as well as the Hidden Markov Modeling and Hilbert-Huang Transform [17,33]. A Bayesian network is adopted in [34] to diagnose the damages in a gear train system, in which six features, including waveform factor, crest, impulse, allowance, kurtosis and skewness, are selected as the damage features as well as the input to the Bayesian network, and six damage classes, namely undamaged baseline, worn gear, broken tooth, rough surface, rough surface with broken tooth, and rough surface with worn gear, are selected as the output of the Bayesian network. The probability terms in the framework in Ref. 34 are obtained via empirical training.

For any realistic SHM application, uncertainty from various sources is inevitable. Lots of effort is expended to suppress the influence from these sources of uncertainty, such as measurement noise, environment fluctuation, operational variability, and other factors from feature estimation algorithms. However, uncertainty always exists in the SHM applications, and quantifying the existed uncertainty makes a different perspective of SHM performance enhancement. Probabilistic models are established in previous research and the analytically derived probability density functions for several transfer-function-based features are given in Ref. 35 and 36. Instead of modeling the likelihood of feature measurement via empirical training, or assuming Gaussian process or Gaussian distributed prediction error, as most people do, this paper takes advantage of available closed-forms of probability density of transformed features, and applies the accurate solution of distribution as the likelihood to a Bayesian recursive model selection process, in order to classify the types/locations of bearing damages. The proposed procedure in this paper employs the updated posterior probability as the selection index, and compared to the traditional accumulated likelihood in diagnosis, the

posterior distinguishes different damage classes in a more sensitive and specific way. Moreover, the posterior evaluated in the Bayesian framework is bounded between 0 and 1, different from the unbounded accumulated likelihood that has only relative meaning from case to case. Ball bearings, as the key component of rotary machines, are focused in this work and multiple bearing damages are successfully classified in terms of maximum posterior. In addition, the adopted Bayesian recursive updating is generic; therefore it may be applied to any classification applications if the feature likelihood is available. The rest of this paper is organized as follows: section 2 will sketch the theoretic framework of the Bayesian damage classification procedure, and section 3 will apply the framework on a rotary machine test-bed. In section 4, a brief summary will be given to conclude the paper.

2. Bayesian Damage Classification via FRF Features

Bayes' theorem describes the relation between prior probability and posterior probability via the likelihood of data observation. In the context of SHM, there is always a confidence level regarding the system status before and after analyzing acquired data. Specific to the problem of damage classification, multiple choices of the system status are pre-defined, and the goal is to make the correct decision among the choices, such as undamaged/damaged condition (a simple binary decision) or what type of damage (regression or in the discrete case, classification). In the context of in-situ SHM, data are collected in a sequential fashion and so does feature evaluation. Any prior confidence of the system status (even uninformed representations of prior information) simply gets modified by the feature likelihood (based on the most current data set) to result in a posterior probability, which can then be used as a prior information probability for the next iteration.

Equation (1) illustrates the Bayesian model selection process in the mathematical way:

$$p\left(\mathcal{M}_j \mid \mathcal{D},\mathbf{M}\right)=\frac{p\left(\mathcal{D} \mid \mathcal{M}_j\right) p\left(\mathcal{M}_j \mid \mathbf{M}\right)}{p\left(\mathcal{D} \mid \mathbf{M}\right)}, \tag{1}$$

in which $p\left(\mathcal{M}_j \mid \mathbf{M}\right)$ is the prior confidence of selecting the *j*-th model from the entire pool **M**, and $p\left(\mathcal{M}_j \mid \mathcal{D},\mathbf{M}\right)$ is the updated posterior given data $\mathcal{D}$ observed. In more detail, the prior describes the confidence or the probability of condition $\mathcal{M}_j$ before testing results or observations are acquired, and the posterior is the updated confidence of $\mathcal{M}_j$ being true after informed by the particular collected data. The data term $\mathcal{D}$ here is a general representation for all the information acquired from the monitoring, and it may refer to the raw time series, as well as the SHM features transformed from the original raw signal. In the rest of this paper, $\mathcal{D}$ will be referred as the processed features, although raw signals could be used as the "data", $\mathcal{D}$, to update the confidence.

In Equation (1), $p\left(\mathcal{D} \mid \mathcal{M}_j\right)$ is the likelihood of observing $\mathcal{D}$ given the *j*-th model $\mathcal{M}_j$ is true. The denominator of Equation (1) is called total evidence for feature set $\mathcal{D}$, since it is the likelihood of $\mathcal{D}$ under all possible situations contained in **M**, as expressed in Equation (2) for a discrete model space:

$$p\left(\mathcal{D} \mid \mathbf{M}\right)=\sum_{j=1}^{n} p\left(\mathcal{D} \mid \mathcal{M}_j\right) \cdot p\left(\mathcal{M}_j \mid \mathbf{M}\right), \tag{2}$$

where *n* is the dimension of the ensemble **M** of all model classes being considered in the classification.

For in-situ damage classification, the model space **M** is interpreted as the superset of all possible damage types and/or locations (all the possible discrete labels that need to be identified), and $\mathcal{M}_j$ is therefore the *j*-th choice of the damage classes. The data observation and/or extracted features, expressed as $\mathcal{D}$ in Equation (2)

are acquired and evaluated in an online fashion, as mentioned. Thus, Equation (1) may be evaluated in a recursive way, such that the posterior probability from the previous step becomes the prior in the next step. Once the data sample is available and its likelihood is evaluated, the confidence is updated and output as the new posterior of this iteration. If there is a consistent partition of the classification space and information to support the decision-making is (at least weakly) stationary, the posterior $p\left(\mathcal{M}_j \mid \mathcal{D},\mathbf{M}\right)$ will tend towards unity (highly plausible) or zero (implausible) as the number of iterations is sufficient. The initial value of the prior is not critical, since the updating process will adjust the inaccuracy from any naïve guess at the very beginning, provided the prior at least spans the classification space. The saturation of posterior confidence to unity or zero indicates the acceptance or rejection of the *j*-th model candidate, i.e., the most plausible damage label in the context of SHM.

This recursive flow is applicable for any type of classification in general, and the scope of this paper is to demonstrate the process via SpectraQuest® Machinery Fault Simulator (MFS) test-bed, using frequency response features evaluated from vibration data. The frequency response function (FRF), also known as the transfer function in a generic context, fully characterizes the (linear) system input-output dynamics in the frequency domain, and the strong physical meaning makes it a fundamental feature in the applications of system identification and SHM. During the operation of rotary machinery, noise and environmental variability will contaminate the signal quality and degrade the FRF estimations. Therefore, designed algorithms—often called estimators—are adopted to minimize the uncertainty effects. The selection among estimators is a technical issue, and is often implemented based on whether input or output has the better quality of signal. There are two estimators listed in Equation (3), called H_1 and H_2 estimators,

$$\hat{H}(\omega)=\underbrace{\frac{\hat{G}_{xy}(\omega)}{\hat{G}_{xx}(\omega)}}_{H_1}=\underbrace{\frac{\hat{G}_{yy}(\omega)}{\hat{G}_{yx}(\omega)}}_{H_2}, \tag{3}$$

in which $\hat{G}_{xx}$, $\hat{G}_{xy}$, $\hat{G}_{yx}$ and $\hat{G}_{yy}$ stand for the auto- and cross-power density function estimations between corresponding signals *x* (input measurement) and *y* (output measurement), and the caret (ˆ) sign denotes the smoothed spectral estimations instead of the true values. These smoothed estimations are often obtained via Welch's averaging method [37], which has become a standard step in real applications to reduce incoherent noise to enhance the quality of the power density and FRF estimations. Using cross-power density $\hat{G}_{xy}$ as example, Equation (4) shows the detail of Welch's averaging:

$$\hat{G}_{xy}(\omega)=\frac{1}{n_d}\sum_{k=1}^{n_d}\tilde{X}_k^*(\omega)\cdot\tilde{Y}_k(\omega), \tag{4}$$

in which the original time series *x* and *y* are split into n_d segments, or repeating *x* and *y* measurements for n_d times, and the discrete Fourier transform (DFT) of each segment is calculated, denoted by $\tilde{X}_k$ and $\tilde{Y}_k$. The ˜ sign denotes the estimation of each individual segment before averaging, and * denotes the complex conjugate. Averaging across all the individual estimations forms the smoothed power spectral estimation in Equation (4). By adopting the Welch's algorithm illustrated in Equation (4), the estimations of power spectra are not only smoothed (by eliminating unbiased "noise"), but also regularized towards an increasingly Gaussian-distributed random variables according to the central limit theorem. This paper will adopt the probabilistic uncertainty quantification models established in [35], and employ the models to describe likelihood of data sample from each iteration. At an arbitrary frequency line ω, the probability density function of the FRF magnitude at the *j*-th condition, as a random variable, is described as:

$$p_{|\hat{H}|}(h \mid \mathcal{M}_j) = \frac{\gamma_j}{\pi\alpha_j} \cdot e^{-\frac{1}{2(1-\rho_j^2)}\left(\frac{\mu_{A_j}^2}{\sigma_{A_j}^2} - 2h\frac{\mu_{A_j}\mu_{C_j}}{\sigma_{A_j}\sigma_{C_j}} + \frac{\mu_{C_j}^2}{\sigma_{C_j}^2}\right)} + \frac{\beta_j}{\sqrt{2\pi}\alpha_j^{3/2}} \cdot e^{-\frac{\left(h\mu_{A_j} - \mu_{C_j}\right)^2}{2\alpha_j}} \cdot \mathrm{Erf}\left(\frac{\beta_j}{\sqrt{2\alpha_j}\gamma_j}\right), \tag{5}$$

in which:

$$\mathcal{M}_j \in \mathbf{M},$$

$$\alpha_j = h^2\sigma_{A_j}^2 - 2\rho_j h\sigma_{A_j}\sigma_{C_j} + \sigma_{C_j}^2,$$

$$\beta_j = h\sigma_{A_j}\left(\rho_j\mu_{A_j}\sigma_{C_j} - \mu_{C_j}\sigma_{A_j}\right) + \sigma_{C_j}\left(\rho_j\mu_{C_j}\sigma_{A_j} - \mu_{A_j}\sigma_{C_j}\right),$$

$$\gamma_j = \sqrt{1-\rho_j^2}\sigma_{A_j}\sigma_{C_j},$$

$$\rho_j = \frac{\mathrm{cov}\left(g_{A_j}, g_{C_j}\right)}{\sigma_{A_j}\sigma_{C_j}},$$

and $\mathrm{Erf}(\cdot)$ is the error function. The order statistics μ_{C_j}, μ_{A_j}, $\sigma_{C_j}^2$, $\sigma_{A_j}^2$ are the mean and variance of $\left|\hat{G}_{xy}\right|$ and $\left|\hat{G}_{xx}\right|$, respectively, at the *j*-th damage condition, and all are frequency-dependent. For the sake of brevity, the frequency variable ω is omitted in the equation. The subscripts *C* and *A* in the order statistics stand for the quantities about Cross- and Auto-power estimations, i.e. $\left|\hat{G}_{xy}\right|$and $\left|\hat{G}_{xx}\right|$.

For the phase estimation of FRF, Equation (6) gives the probability density function at the *j*-th condition:

$$p_{\angle\hat{H}}(\theta \mid \mathcal{M}_j) = \frac{e^{-\frac{\mu_{R_j}^2 + \mu_{I_j}^2}{2\sigma_j^2}}}{2\pi} + \frac{\eta_j \cdot e^{-\frac{\left(\mu_{R_j}\sin(\theta) - \mu_{I_j}\cos(\theta)\right)^2}{2\sigma_j^2}}}{2\sqrt{2\pi}\sigma_j}\left(1 + \mathrm{Erf}\left(\frac{\eta_j}{\sqrt{2}\sigma_j}\right)\right), \tag{6}$$

in which $\eta_j = \mu_{R_j}\cos(\theta) + \mu_{I_j}\sin(\theta)$, and μ_{R_j} and μ_{I_j} are the mean of real and imaginary parts of FRF, $\hat{H}_{R_j}$ and $\hat{H}_{I_j}$, and σ_j^2 is the variance of both parts.

Equation (5) and Equation (6) characterize the distributions of single sample of FRF magnitude and phase estimations using an H_1 estimator, and for H_2 estimator, the PDF will be the same form but switch the coefficients for the numerator and denominator. Consider a consecutive N-sample data set: $\mathcal{D}_{1:N} = \{z_i, i = 1,2,3...q, q+1...N\}$, the likelihood term in Equation (1) on the q-th iteration may be evaluated as:

$$p(\mathcal{D}_{1:q} \mid \mathcal{M}_j) = \prod_{i=1}^{q} \Theta(z_i \mid \mathcal{M}_j). \tag{7}$$

in which Θ and z are the common notations of probability density function and its sample variable expressed in Equation (5) and Equation (6). Equation (7) assumes all feature samples are independent, so the total likelihood is therefore the product of individual sample likelihoods. Although there are inherent dynamics which makes the samples possibly correlated with each other, the independence assumption here works fine in practical implementation. This is primarily due to the relative influence from system dynamics compared to the influence from the randomness. In fact, in the time scale of sampling interval, the correlation between samples due to the system dynamics is negligible, and uncertainty dominates the sampling at this scale, resulting in Equation (7) being satisfied favorably. The same argument may be made in regard to the stationarity and spectral characteristics of time series measurement. Despite of the mathematical requirements of stationarity and normality in the statistical modeling of Equation (5) and (6), the work in this article shows the applicability of those uncertainty quantification models to a non-ideal situation, in which the acquired data are non-stationary in a short time scale and colored in the spectral domain.

By evaluation the likelihood of data observation in Equation (7), damage labels may be determined directly as the candidate with the maximum likelihood. In the next section, Bayesian recursive classification will be conducted as structured in Equation (1), or more explicitly as Equation (8):

$$p\left(\mathcal{M}_j \mid \mathcal{D}_{1:q}, \mathbf{M}\right) = \frac{\left[\prod_{i=1}^{q} \Theta\left(z_i \mid \mathcal{M}_j\right)\right] p\left(\mathcal{M}_j \mid \mathcal{D}_{1:q-1}, \mathbf{M}\right)}{p\left(\mathcal{D}_{1:q} \mid \mathbf{M}\right)}, \tag{8}$$

and the performance will be compared to the approach with only the likelihoods involved.

3. Experimental Implementation of Damage Classification

In this section, the proposed Bayesian classification framework is deployed on the SpectraQuest® Machinery Fault Simulator (MFS), where multiple types of damages occur on the ball bearing at the right-hand-side shaft support, as shown in Figure 1. The system runs at the speed of 1000 rpm, with a 5 kg radial loader near the test bearing to enhance the spectral magnitude in the response. Acceleration signals are acquired with a sampling rate of 10 kHz in the directions *y* (horizontal radial) and *z* (vertical radial) via National Instruments™ 9402 I/O module. In addition to the undamaged baseline condition ($\mathcal{M}_1$), two more cases with damages on balls ($\mathcal{M}_2$) and the outer race ($\mathcal{M}_3$) are included, as illustrated in Figure 2. This makes the problem a trinary classification, i.e. $\mathbf{M} = \left\{\mathcal{M}_j, j = 1,2,3\right\}$. FRFs for different damaged conditions are estimated based upon the acceleration data, with respect to the power spectra in the two directions *y* and *z*.

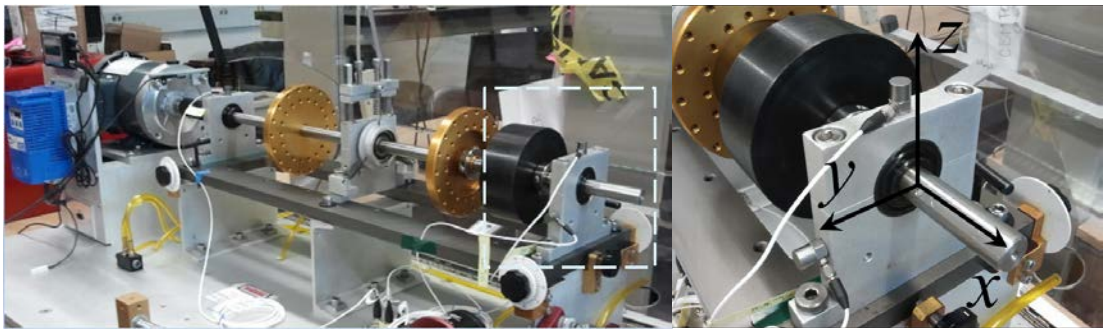

Figure 1: SpectraQuest® Machinery Fault Simulator (MFS) test-bed

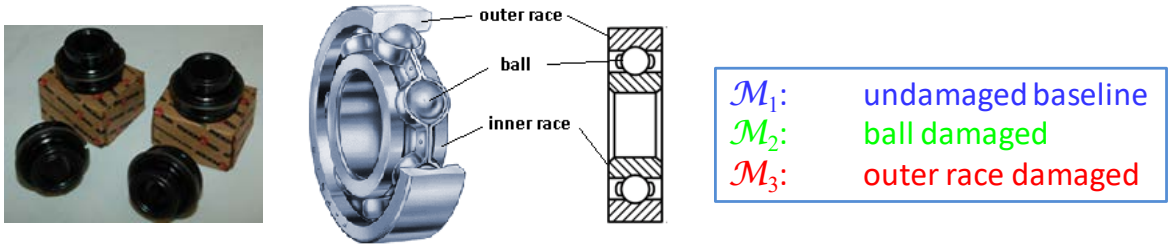

Figure 2: Ball bearings in the system and damages to be classified

Figure 3 and Figure 4 plot the FRFs for each damaged conditions. The averages on the left are calculated via averaging all the data sets, i.e. after all iterations/samples are collected. On the right, observation of each iteration/sample, i.e. realization in the context of statistics, is plotted as well as a zoom-in view. In Figure 3 and Figure 4, a lot of realizations from different damaged conditions overlap significantly, leading to a very poor distinguishability. Without a specialized classifier, only very vague classification decisions would be made even if a large cluster of realizations are available.

As addressed previously, uncertainty in the feature estimations are characterized at each single frequency line via Equation (5) and Equation (6); according to Figure 3 and Figure 4, not all frequencies yield the same distinguishability of data clusters. As an example, Figure 5 plots the distributions of magnitude and phase features at an arbitrarily selected frequency line near 3.5 kHz, and despite the overlap between distributions, the statistical patterns are quite different. Additionally, because circular phase is a periodic function, the tails of its distribution do not vanish at the $\pm\pi$ boundaries, but smoothly connect at the wrapping point.

Given the probability of each sample falling into different statistical models, the likelihood of entire historical data observation is calculated in Equation (7), and the Bayesian recursive process may be conducted according to Equation (8). As mentioned previously, the initial setting of prior confidence before any knowledge from data observations is not critical, as the Bayesian recursion will correct the final posterior according to likelihood seeing the data series. Particularly in the trinary damage classification of the MFS test-bed, the prior confidence of selecting $\mathcal{M}_1$ is set to be 80%, indicating more initial confidence that the system is undamaged. For setting the prior of selecting $\mathcal{M}_2$ and $\mathcal{M}_3$ among the remaining chance, which is 20%, no initial preference will be given in this section, and the priors are initially set at 10% for both cases.

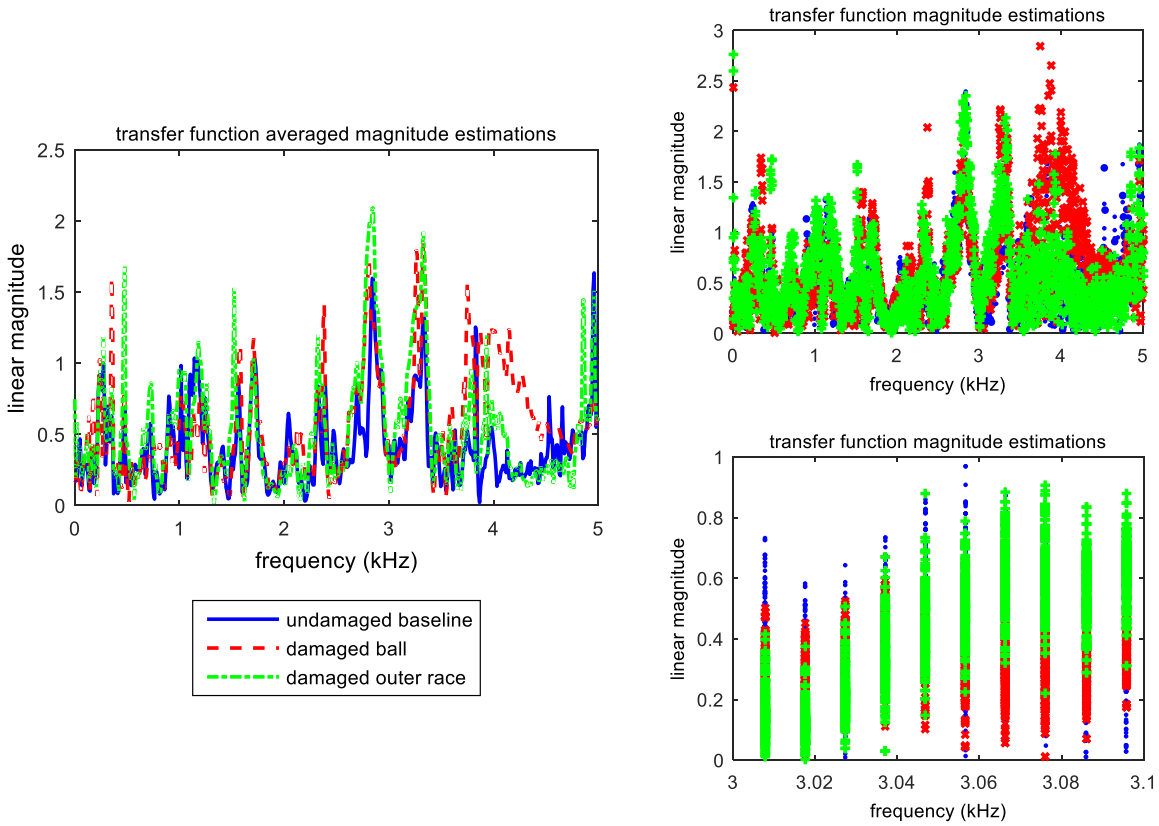

Figure 3: FRF magnitude average and multiple samples

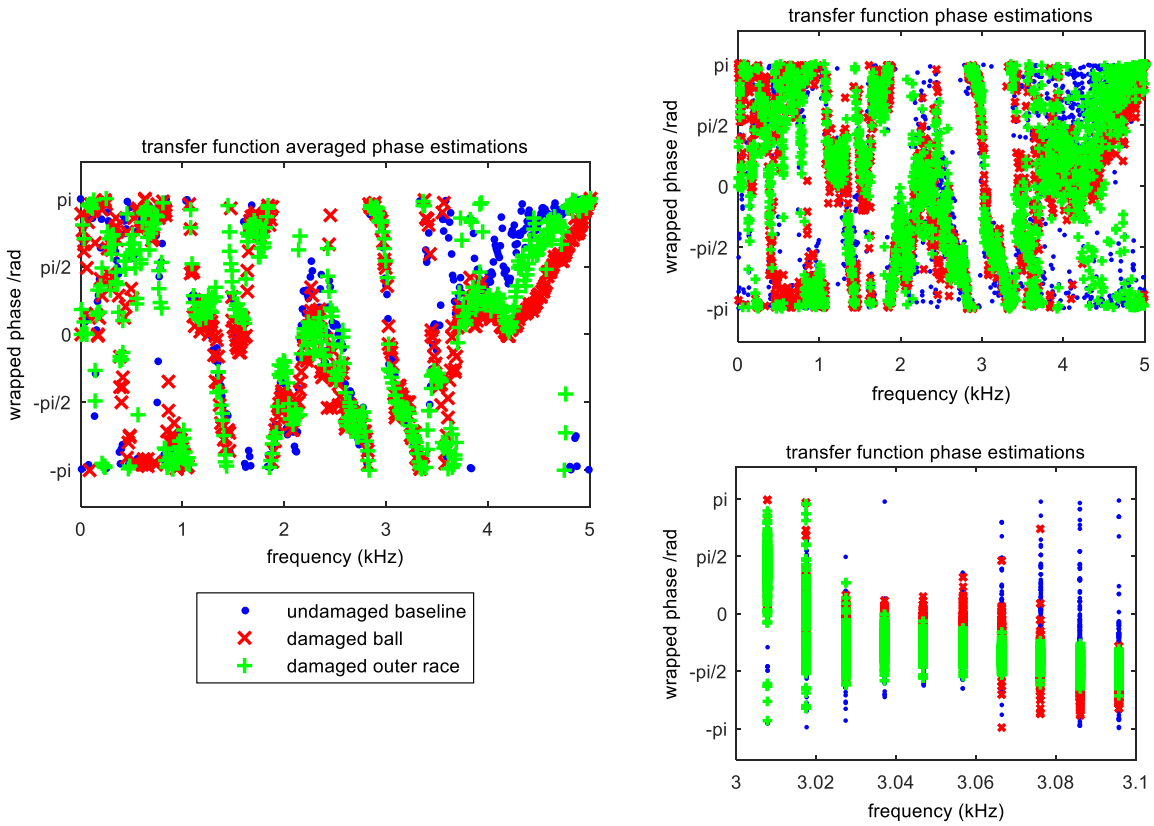

Figure 4: FRF phase average and multiple samples

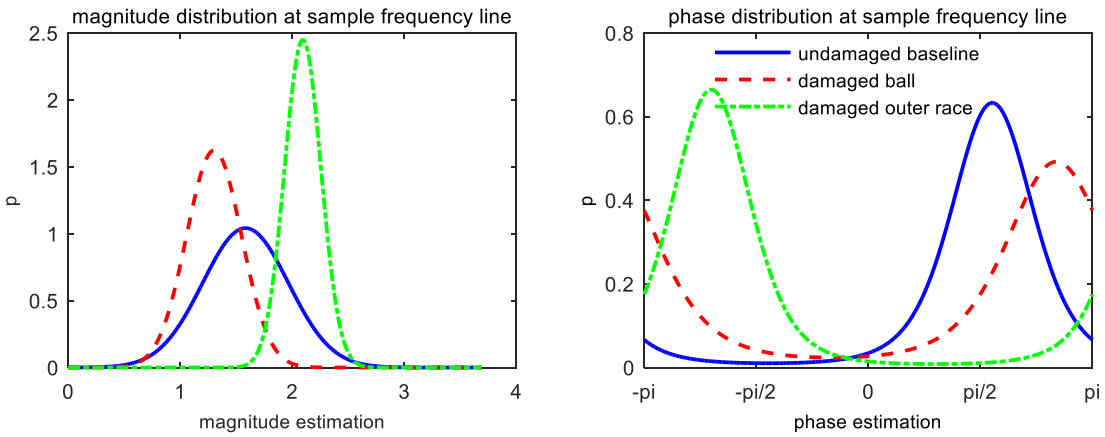

Figure 5: PDFs of different damage cases at an arbitrary frequency line near 3.5 kHz

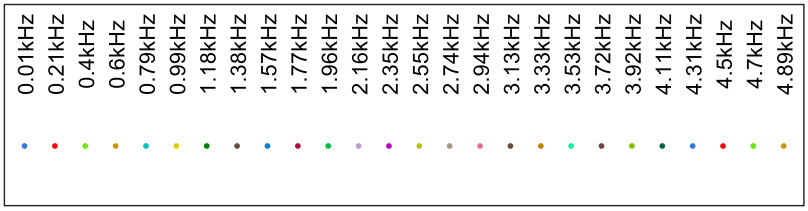

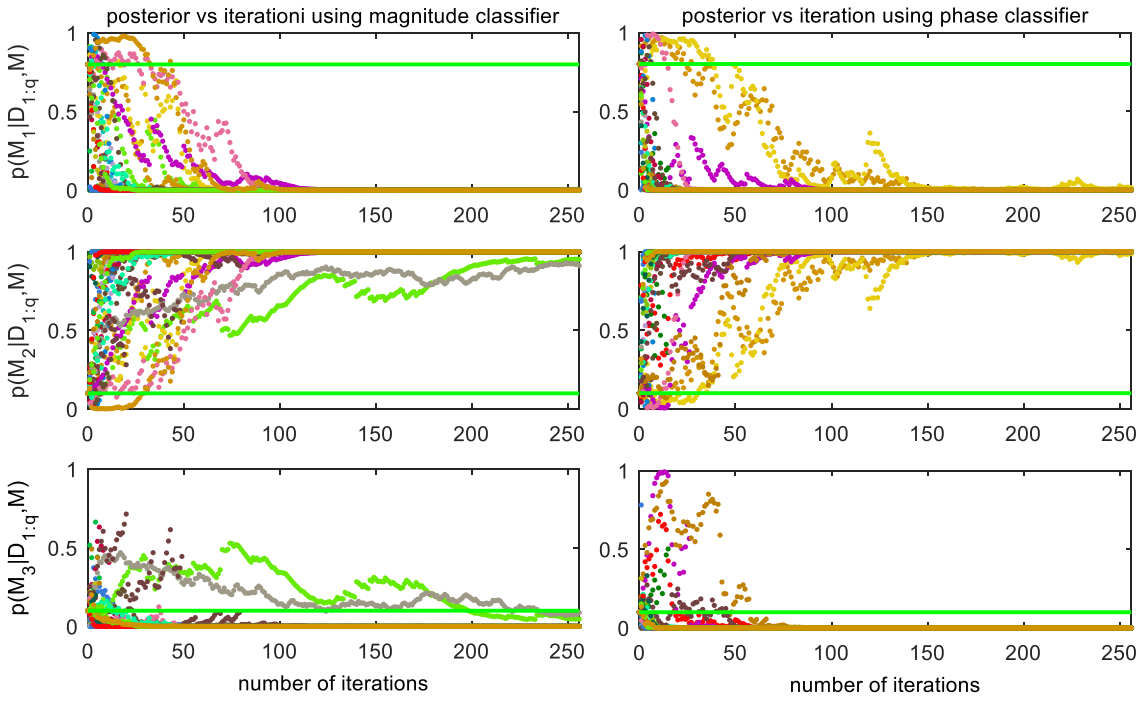

Figure 6: Posterior of selecting $\mathcal{M}_1$ (top), $\mathcal{M}_2$ (middle) or $\mathcal{M}_3$ (bottom) at each iteration, given $\mathcal{M}_2$ is true

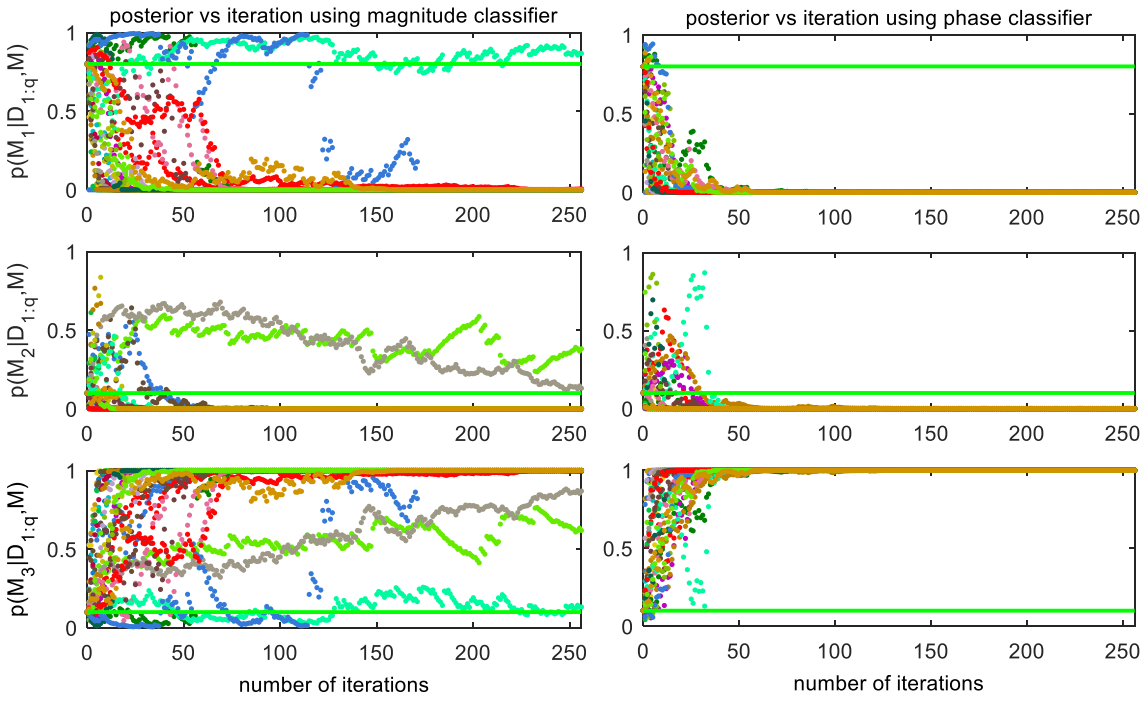

Figure 7: Posterior of selecting $\mathcal{M}_1$ (top), $\mathcal{M}_2$ (middle) or $\mathcal{M}_3$ (bottom) at each iteration, given $\mathcal{M}_3$ is true

Figure 6 and Figure 7 plot the outcome of the Bayesian recursive updating process as a function of iteration, i.e., the posteriors of selecting the damage types $\mathcal{M}_1$ (top), $\mathcal{M}_2$ (middle) and $\mathcal{M}_3$ (bottom), given that $\mathcal{M}_2$ or $\mathcal{M}_3$ is true, respectively. Results are shown for both FRF magnitude and phase features, and results at multiple frequency lines are also included as indicated by different markers. These frequency lines, as examples, are randomly picked with even intervals (1 picked every 10 frequency bins out of 256 total) in the frequency domain (up to 5 kHz Nyquist), and all selected frequencies are listed on top of Figure 6. From the two clusters of figures, it is obvious that starting from an arbitrary initial prior, plotted as the horizontal bar, the posterior probability is updated on every iteration, and for most of the frequency lines, it converges to

either unity or zero after tens of iterations. The algorithm outputs unit posterior to accept the class, and zero to reject the class, as illustrated in Figure 6 and Figure 7. Considering the speed of the convergence, there are frequencies at which the convergence is rapid, but a few of them show obvious slow convergence, without saturation after 250 iterations. The different rates of converging are primarily due to the distinguishability of the problem itself, such as the specific vibrational nature of the changes induced by the various damage labels, as well as the external noise contamination. In other words, there is usually good signal quality at resonances which will lead to good distinguishability if the nature of damages will also cause different patterns of change, and on the other hand, the poor capability of classification at certainty frequency is the result of some combination of less-representative features and low signal-to-noise ratio at that frequency. A particular frequency line of the magnitude classifier in Figure 7 explains the converging rate clearly, at which the posteriors of selecting each model candidate do not change much deviating from the arbitrarily-set initial prior. This indicates that the data $\mathcal{D}$ do not supply any useful information to support/deny any possible damage types, and this may be due to the poor signal-to-noise ratio as well as the insensitivity to the damages at this particular frequency as abovementioned.

Figure 8 and Figure 9 demonstrate the ensemble averages of logarithmic likelihood and posterior among all the frequency lines as a function of number of iterations. In each figure, the four subplots represent the two damage types (damaged ball and outer race) and the two classifying features (FRF magnitude and phase). From the curves illustrated in Figure 8, the logarithmic likelihoods for the data observation under anyone of the three damage classes increase monotonically, and near-linearly, although the correct model always has the highest likelihood. Since all logarithmic likelihood curves have a near-linear characteristic and all of them go up as more iterations are included, the distinguishability of different classes is all dependent on the slope

difference and number of iterations. In other words, the classification via likelihood will only have good performance when the number of iterations is sufficient, or the slope of logarithmic likelihood progression is significant, so that the values at the end of the curves will be dramatically differentiable. On the contrary, the curves given by Figure 9 show a better approach, as the curves for correct and wrong decisions go in the opposite direction, and after 30 to 50 iterations, the posteriors are fully distinguished as almost unity and zero. Compared to the classification based on likelihood, the Bayesian recursive process outperforms, in terms of the curve trend and lower necessary number of iterations. Moreover, the Bayesian posterior is always bounded between 0 and 1, so the nearness/farness from an extreme can always be quantifiably understood. On the contrary, accumulated likelihood does not have mathematical limits as references, and the selection is made merely via relative difference from class to class.

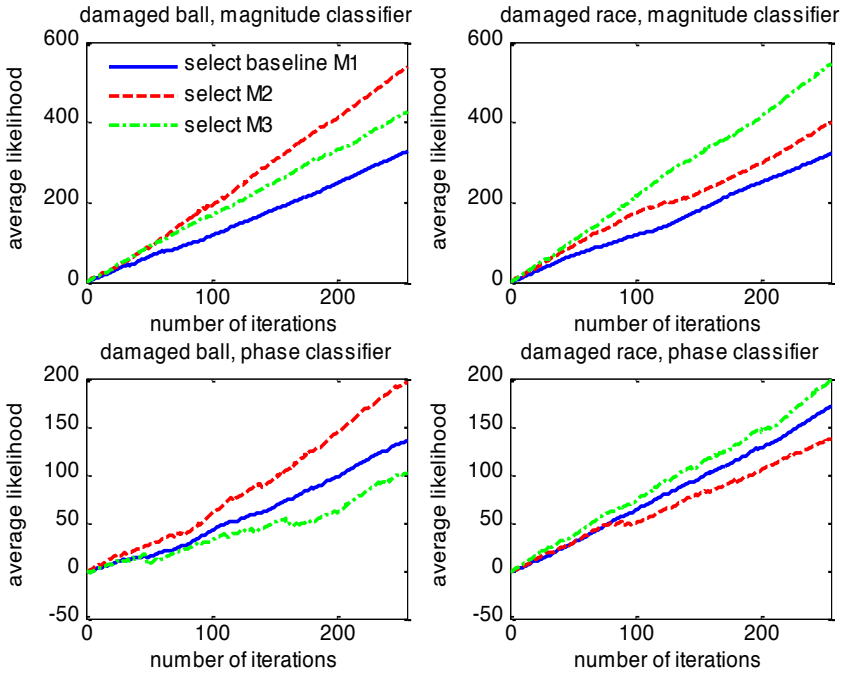

Figure 8: Average likelihood of selecting each candidate vs. number of iterations

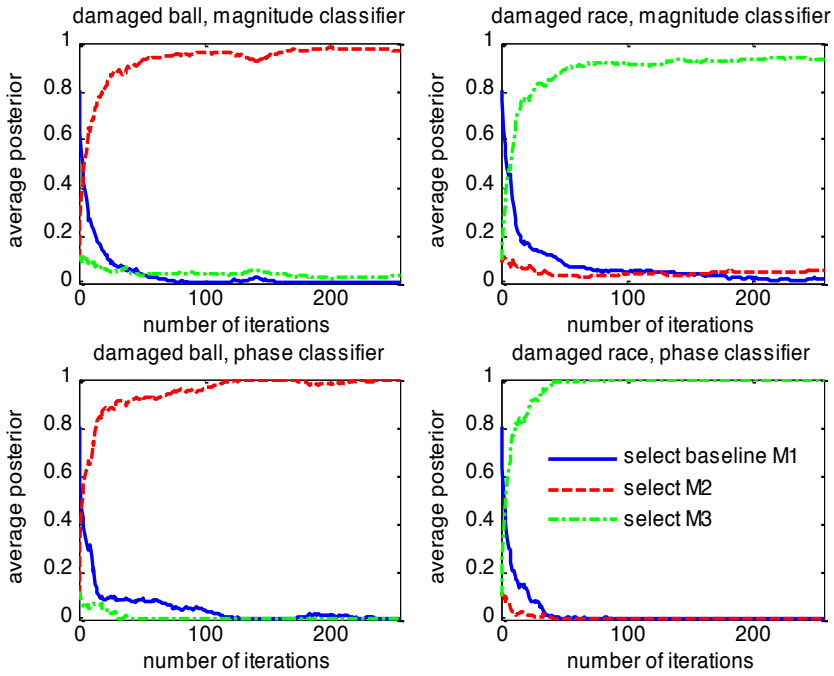

Figure 9: Average posterior of selecting each candidate vs. number of iterations

In these experiments, there are 250 rounds of feature evaluations from the data acquired from the MFS test-bed, and Figure 9 just shows how the decision is made in a more decisive manner as the information is accumulated from the data set. After all the data set is acquired, a more straightforward illustration is available in Figure 10, which compares the final values of averaged likelihood and posterior for each of the testing conditions and classifiers.

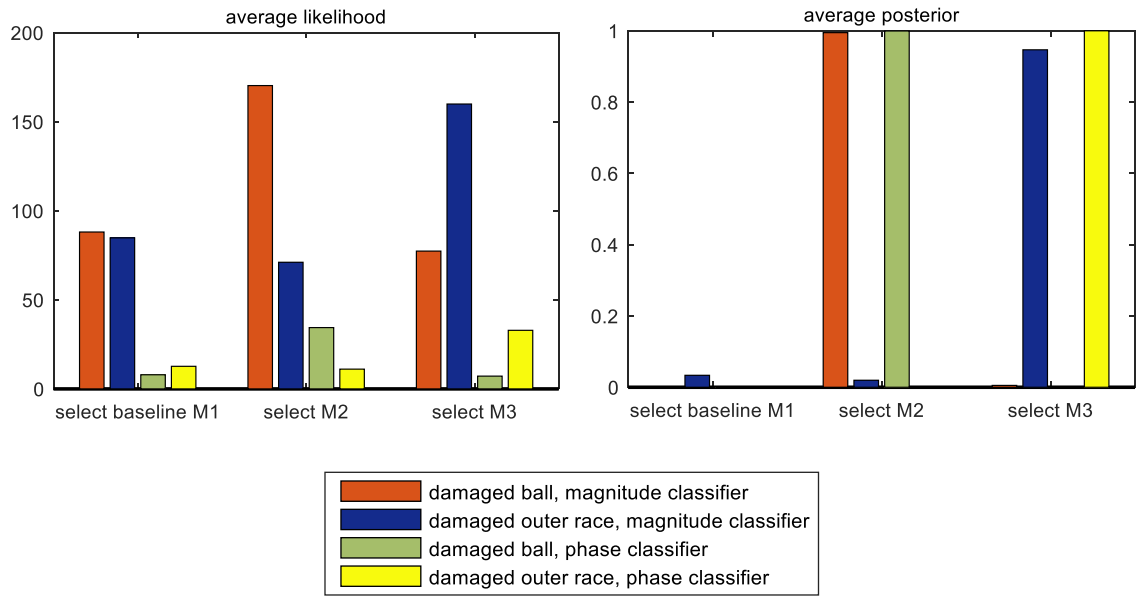

Figure 10: Average likelihood and posterior after 250 iterations of selecting each candidate

In Figure 10 there are three clusters of bars representing the likelihood and posterior of selecting among $\mathcal{M}_1$, $\mathcal{M}_2$ and $\mathcal{M}_3$, using magnitude and phase classifiers, when in reality the ball or outer race is damaged. Consistent with the previous analysis, both likelihood and posterior classify the two types of damage correctly, using both magnitude and phase features. In the figure, the average posterior gives the correct classification in a much more significant way, and compared to the bars in the plot on the left-hand-side, the posterior confidence of selecting the correct class is close to unity with only negligible probabilities suggesting selecting one of the other two wrong classes.

The implementation of Bayesian recursive damage classification as a model selection process on the MFS test-bed is conducted in a well-controlled laboratory environment. However, in real SHM applications, the

uncertainty from numerous sources undoubtedly degrades the performance further, and causes lots of ambiguity in interpreting SHM features and making decisions. In the rest of this section, a more rigorous situation will be considered to validate the framework, and 20% of white noise contamination in terms of noise-to-signal ratio will be added artificially to the original lab-acquired vibration data, in order to simulate a harsher operational environment.

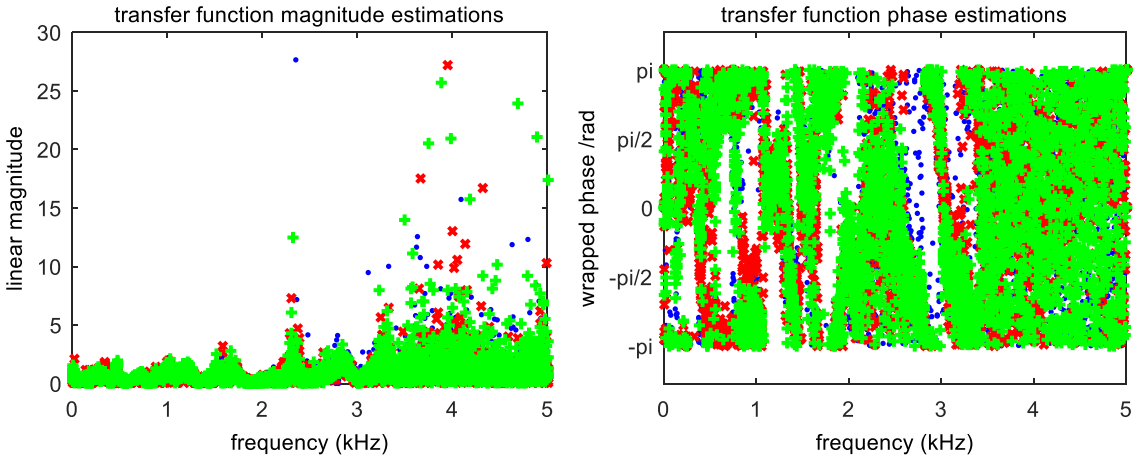

Figure 11: FRF magnitude and phase estimations with contaminated data

Figure 11 illustrates the magnitude and phase estimations for all three conditions. Compared to Figure 3 and Figure 4, the estimations with noise contamination are much more dispersed and random, and the contamination also makes the classification impossible at any frequency just by looking at the features (the so-called “viewgraph norm”). Figure 12 plots the feature distributions at the same sample frequency as shown in Figure 5, and the curves show not only wider distributing range but also more overlap among the damage labels. Implementing the same flow described in Equation (8), the updated posteriors versus the number of iterations are plotted in Figure 13 and Figure 14, in which the clusters of posterior of selecting each damage

class, given ball or outer race damaged, are plotted as function of iteration number. Similar to the non-contaminated case, given an arbitrary initial prior, the posterior evaluated at a large number of frequencies converges to the selection of correct model. However, there are more frequency lines that have poor classification power. At some of these lines, the posteriors take more iterations to converge, but some of them will oscillate and even converge erroneously. Those frequencies with poor performance are the evidence of how noise contamination degrades the decision-making, because the feature evaluation at those frequencies is primarily dominated by the noise/uncertainty without useful information.

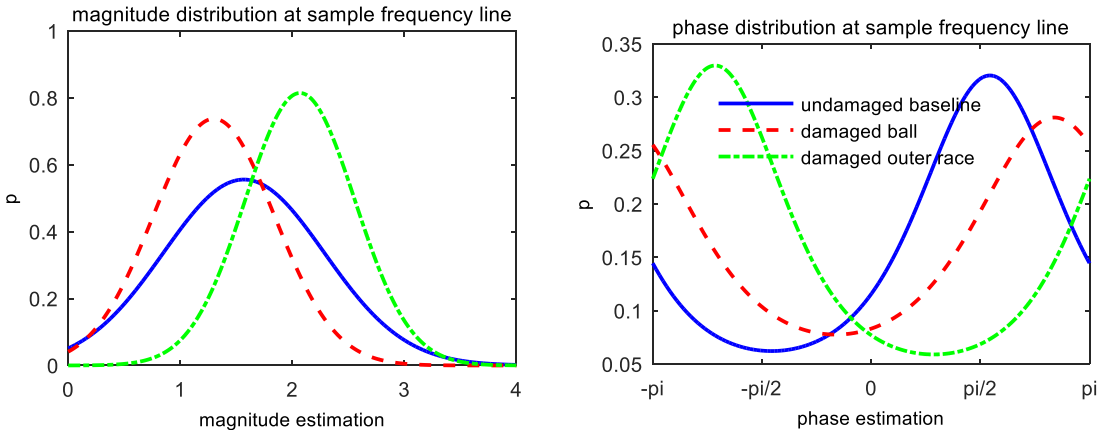

Figure 12: PDFs of different damage cases at an arbitrary frequency line near 3.5 kHz with contaminated data

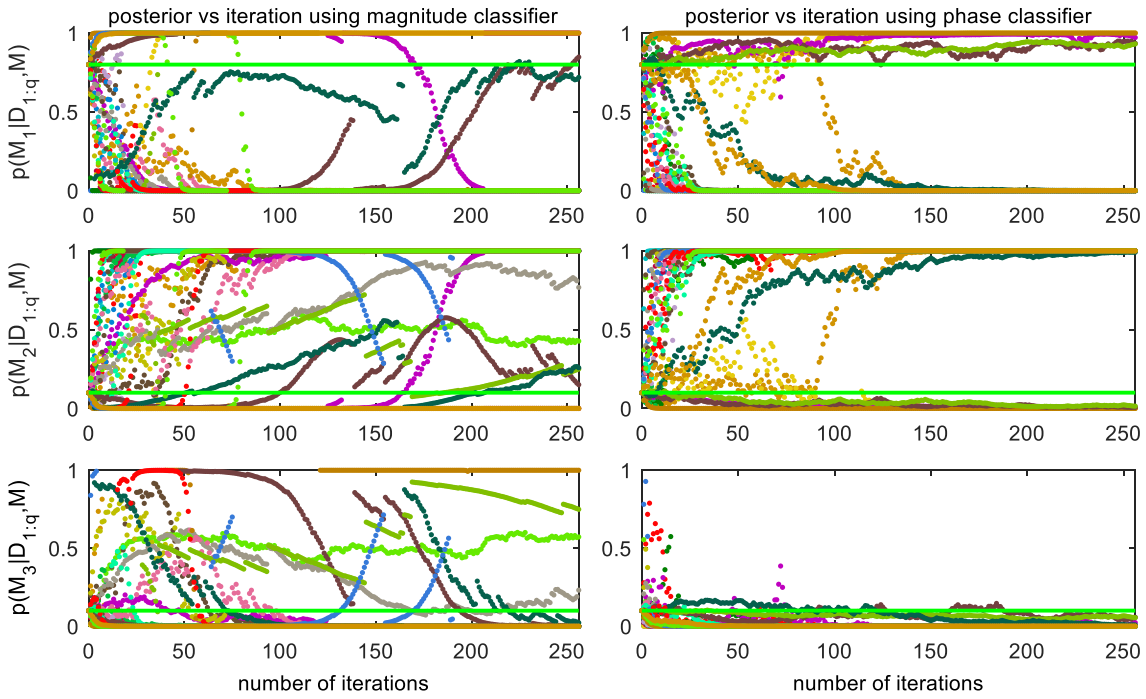

Figure 13: Posterior of selecting $\mathcal{M}_1$ (top), $\mathcal{M}_2$ (middle) or $\mathcal{M}_3$ (bottom) at each iteration, given $\mathcal{M}_2$ is true, with contaminated data

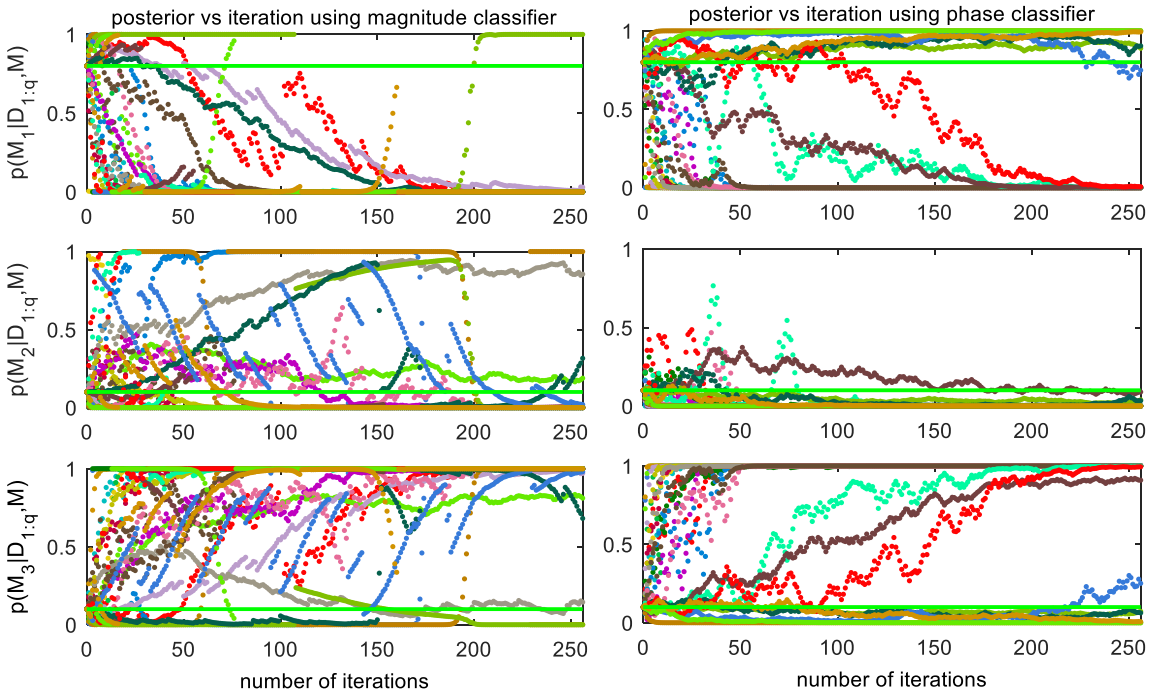

Figure 14: Posterior of selecting $\mathcal{M}_1$ (top), $\mathcal{M}_2$ (middle) or $\mathcal{M}_3$ (bottom) at each iteration, given $\mathcal{M}_3$ is true, with contaminated data

Averaging the logarithmic likelihood and posterior curves across all the frequencies results in the plots shown in Figure 15 and Figure 16. From Figure 15, the separation of classes is still poor (if not worse), as expected, and with a small number of iterations, those curves may be entangled leading to an incorrect classification. The phase classifier in classifying the two damages shows a little enhancement as the curves for right and wrong model selections go to different direction, but this observed opposite direction happens randomly and is only specific for this experiment, as the influence from contamination is complicated and changes of uncertainty characteristics, such as signal-to-noise ratio, will affect the trend in an unapparent way.

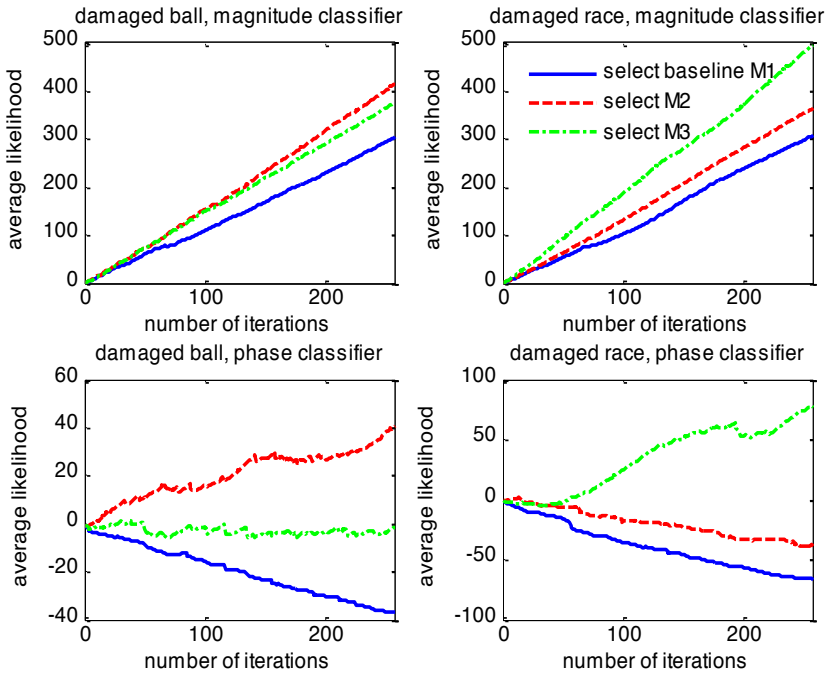

Figure 15: Average likelihood of selecting each candidate vs. number of iterations with contaminated data

The contamination also degrades the performance of Bayesian recursive approach, but the same as non-contaminated case, the curves for selecting right and wrong types converge to opposite directions. The curves for the contaminated case contain more variability and poorer convergence, in terms of converging time and final asymptotic confidence.

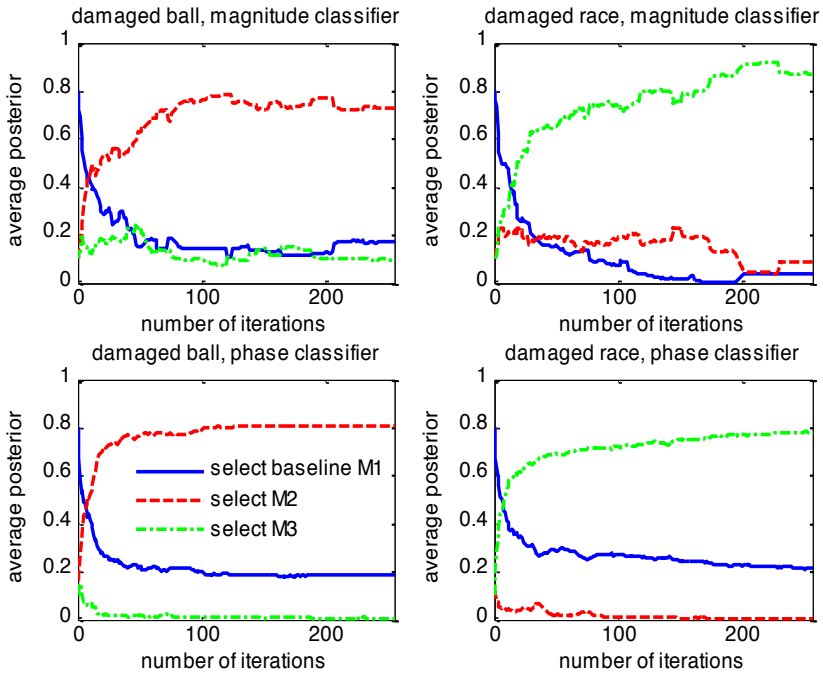

Figure 16: Average posterior of selecting each candidate vs. number of iterations with contaminated data

Comparing the two decision makers, i.e. likelihood and Bayesian posterior, Figure 17 compares the final averaged value with extraneous noise contamination, after the entire 250 realizations have been acquired. The similar conclusion may be drawn that the posterior provides a much more confident decision, appropriately quantified.

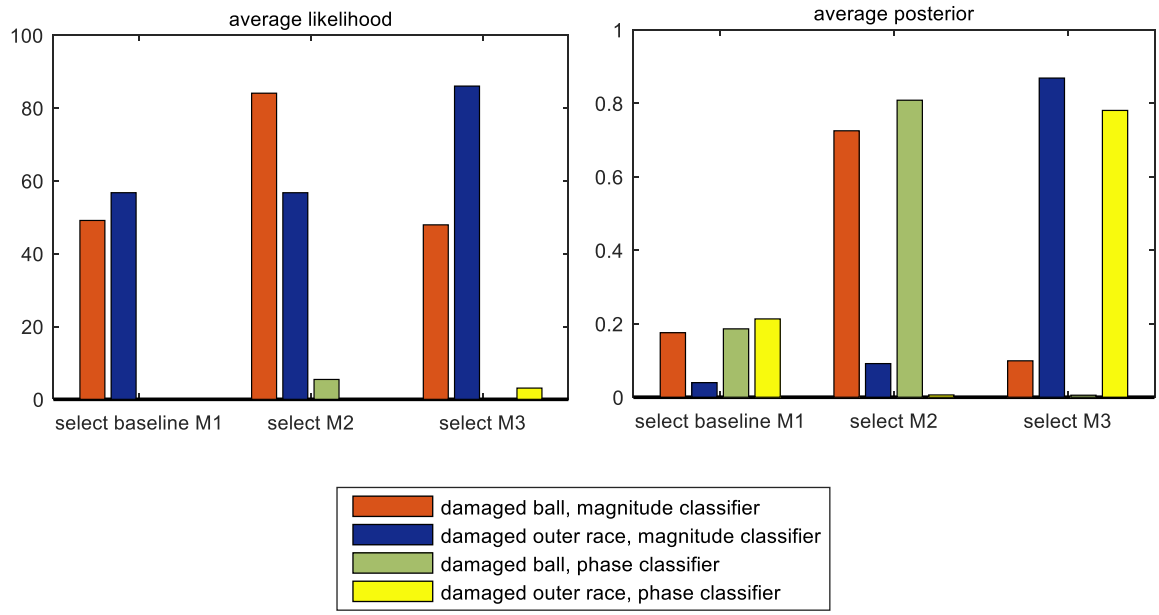

Figure 17: Average likelihood and posterior after 250 iterations of selecting each candidate with contaminated data

4. Conclusion

This paper adopts the Bayesian recursive framework to identify ball bearing damage types/locations via the proposed model selection procedure. FRF magnitude and phase evaluated from the acquired vibrational data are selected as the SHM features. Instead of an empirical or Gaussian-related likelihood model, the likelihood term in the Bayesian framework presented in this paper is built up analytically, based on the closed-form probabilistic uncertainty quantification models established previously. Confidence of the decision, i.e. the types and locations of the damage, is updated recursively via the likelihood of the feature observations, and

therefore the damage classification decision is made to the damage class with the maximum posterior probability. A damage classification flow is generalized as flows:

- Discretize the damaged conditions, such as types, severities and locations, into finite states
- Obtain information from each of the states as a training process
- Establish probabilistic uncertainty quantification model of the extracted SHM feature
- Evaluate the likelihood of data acquired from in-situ testing with unknown status
- Apply the Bayesian recursive classification process with an initial prior, and update the posterior confidence of each condition candidate

In this algorithm, the idea is to classify the observed information to a category that have previously trained. The ensemble of all the possibilities is a finite set, so the Bayesian classification algorithm picks the most plausible model candidate to explain the observation, which may lead to the most similar case in the training set. When there are more sophisticated damage scenarios, such as a combination of multiple damage types/locations, the finite-state set-up of training sets should be more complicated accordingly, the required training cases gets exponentially increased, and multi-dimensional features should be employed as well to reach a valid classification. Compared to other model-based Bayesian inference approaches, this data-driven flow does not have any computational burden, as all the information is acquired from data observation, rather than a model evaluation.

In the employed MFS test-bed, to demonstrate the recursive framework, two types of bearing damages are included besides the undamaged baseline, namely damaged ball and damaged outer race respectively. The posterior as a function of iterations gives a clear illustration on how the decisiveness is converging to the ideal level within tens of iterations, i.e. for the correct class the posterior converges to unity, and for the incorrect

class not to be selected, the posterior converges to zero. The performance of damage classification via posterior is compared to the hypothesis testing via likelihood, and test results show a significant advantage of adopting the Bayesian recursive process. The likelihood accumulates without actual bounds, so that the likelihood-based model selection is to make decision according to the relative difference between models. For posterior, there is strong statistical interpretation because this probability is bounded between 0 and 1. Therefore, the closeness of posterior to the extremes directly indicates the decisiveness.

To be more realistic, the vibrational data acquired from lab-scale MFS test-bed are contaminated by 20% of artificial white noise, in terms of noise-to-signal ratio. The performance is degraded, unsurprisingly, due to the contamination, for both the classification based on likelihood and posterior, but under this circumstance, the posterior obtained from Bayesian recursive process is still much more sensitive and specific to the damage classification problems.

In this work, the damage classification decisions are made according to a naïve prior and in-situ vibrational data. Due to the nature of the acceleration data acquired from a rotating machinery, the normality and independency are not guaranteed in theory, as the rattling in a damaged gear is highly characteristic and cohered with the system dynamics. However, the work proves that the dependency is ignorable and the influence from previous state to the next state is tiny, nor does the lack of normality in the time series influence the classification for the reason the central limit theorem. Although the likelihood function applied in this work requests multiple mathematical conditions, the applicability of the probabilistic uncertainty quantification model in this Bayesian framework is satisfied.

Acknowledgement

This research was supported by the research grant (UD130058JD) of the Agency for Defense Development of the Korean government and by the Leading Foreign Research Institute Recruitment Program through the National Research Foundation of Korea funded by the Ministry of Science, ICT and Future Planning (2011-0030065).

Reference

1. Worden K, Dulieu-Barton JM. An Overview of Intelligent Fault Detection in Systems and Structures. *Struct Health Monit.* 2004 Mar 1;3(1):85–98.

2. Rytter A. Vibration Based Inspection of Civil Engineering Structures. PhD Thesis, Aalborg University, 1993.

3. Jardine AKS, Lin D, Banjevic D. A Review on Machinery Diagnostics and Prognostics Implementing Condition-Based Maintenance. *Mech Syst Signal Process.* 2006 Oct;20(7):1483–1510.

4. Farrar CR, Worden K. An Introduction to Structural Health Monitoring. *Philos Trans R Soc Math Phys Eng Sci.* 2007 Feb 15;365(1851):303–315.

5. Doebling SW, Farrar CR, Prime MB. A Summary Review of Vibration-Based Damage Identification Methods. *Identif Methods" Shock Vib Dig.* 1998;30:91–105.

6. Farrar CR, Doebling SW, Nix DA. Vibration–Based Structural Damage Identification. *Philos Trans R Soc Lond Math Phys Eng Sci.* 2001 Jan 15;359(1778):131–149.

7. Worden K, Farrar CR, Manson G, Park G. The Fundamental Axioms of Structural Health Monitoring. *Proc R Soc Lond Math Phys Eng Sci.* 2007 Jun 8;463(2082):1639–1664.

8. De Lautour OR, Omenzetter P. Damage Classification and Estimation in Experimental Structures using Time Series Analysis and Pattern Recognition. *Mech Syst Signal Process.* 2010 Jul;24(5):1556–1569.

9. Ni Y-Q, Jiang SF, Ko JM. Application of Adaptive Probabilistic Neural Network to Damage Detection of Tsing Ma Suspension Bridge. *Proc. SPIE 4337, Health Monitoring and Management of Civil Infrastructure Systems*, 2001 August; doi: 10.1117/12.435610.

10. Sohn H, Allen DW, Worden K, Farrar CR. Statistical Damage Classification Using Sequential Probability Ratio Tests. *Struct Health Monit.* 2003 Mar 1;2(1):57–74.

11. Sohn H, Worden K, Farrar CR, Sohn H, Worden K, Farrar CR. Statistical Damage Classification under Changing Environmental and Operational Conditions. *J Intell Mater Syst Struct.* 2002;13:561–574.

12. Chakraborty D, Kovvali N, Wei J, Papandreou-Suppappola A, Cochran D, Chattopadhyay A. Damage Classification Structural Health Monitoring in Bolted Structures Using Time-frequency Techniques. *J Intell Mater Syst Struct.* 2009 Jul 1;20(11):1289–1305.

13. Peng ZK, Chu FL. Application of the Wavelet Transform in Machine Condition Monitoring and Fault Diagnostics: a Review with Bibliography. *Mech Syst Signal Process.* 2004 Mar;18(2):199–221.

14. Peng ZK, Tse PW, Chu FL. A Comparison Study of Improved Hilbert–Huang Transform and Wavelet Transform: Application to Fault Diagnosis for Rolling Bearing. *Mech Syst Signal Process.* 2005 Sep;19(5):974–988.

15. Reda Taha MM, Lucero J. Damage Identification for Structural Health Monitoring using Fuzzy Pattern Recognition. *Eng Struct.* 2005 Oct;27(12):1774–1783.

16. Heng A, Tan ACC, Mathew J, Montgomery N, Banjevic D, Jardine AKS. Intelligent Condition-Based Prediction of Machinery Reliability. *Mech Syst Signal Process.* 2009 Jul;23(5):1600–1614.

17. Bunks C, McCarthy D, Al-Ani T. Condition-Based Maintenance of Machines using Hidden Markov Models. *Mech Syst Signal Process.* 2000 Jul;14(4):597–612.

18. Zhou W, Chakraborty D, Kowali N, Papandreou-Suppappola A, Cochran D, Chattopadhyay A. Damage Classification for Structural Health Monitoring Using Time-Frequency Feature Extraction and Continuous Hidden Markov Models. *Conference Record of the Forty-First Asilomar Conference on Signals, Systems and Computers, 2007.* ACSSC 2007. 2007. p. 848–852.

19. Sohn H, Law KH. A Bayesian Probabilistic Approach for Structure Damage Detection. *Earthq Eng Struct Dyn.* 1997;26(12):1259–1281.

20. Sohn H, Law KH. Bayesian Probabilistic Damage Detection of a Reinforced-Concrete Bridge Column. *Earthq Eng Struct Dyn.* 2000;29(8):1131–1152.

21. Yang Y, Nagarajaiah S. Structural Damage Identification via a Combination of Blind Feature Extraction and Sparse Representation Classification. *Mech Syst Signal Process.* 2014 Mar 3;45(1):1–23.

22. Beck J, Yuen K. Model Selection Using Response Measurements: Bayesian Probabilistic Approach. *J Eng Mech.* 2004;130(2):192–203.

23. Vanik M, Beck J, Au S. Bayesian Probabilistic Approach to Structural Health Monitoring. *J Eng Mech.* 2000;126(7):738–745.

24. Fan Y, Li CJ. Diagnostic Rule Extraction from Trained Feedforward Neural Networks. *Mech Syst Signal Process.* 2002 Nov;16(6):1073–1081.

25. Stack JR, Habetler TG, Harley RG. Fault Classification and Fault Signature Production for Rolling Element Bearings in Electric Machines. *4th IEEE International Symposium on Diagnostics for Electric Machines, Power Electronics and Drives, 2003.* SDEMPED 2003. 2003. p. 172–176.

26. Dyer D, Stewart RM. Detection of Rolling Element Bearing Damage by Statistical Vibration Analysis. *J Mech Des.* 1978 Apr 1;100(2):229–235.

27. Zoubek H, Villwock S, Pacas M. Frequency Response Analysis for Rolling-Bearing Damage Diagnosis. *IEEE Trans Ind Electron.* 2008 Dec;55(12):4270–4276.

28. Staszewski WJ, Worden K, Tomlinson GR. Time–Frequency Analysis in Gearbox Fault Detecting using the Wigner-Ville Distribution and Pattern Recognition. *Mech Syst Signal Process.* 1997 Sep;11(5):673–692.

29. Yan R, Gao RX, Chen X. Wavelets for Fault Diagnosis of Rotary Machines: A Review with Applications. *Signal Process.* 2014 Mar;96:1–15.

30. Cheng J, Yu D, Yu Y. A Fault Diagnosis Approach for Roller Bearings based on EMD Method and AR Model. *Mech Syst Signal Process.* 2006 Feb;20(2):350–362.

31. Widodo A, Yang B-S. Support Vector Machine in Machine Condition Monitoring and Fault Diagnosis. *Mech Syst Signal Process.* 2007 Aug;21(6):2560–2574.

32. Widodo A, Kim EY, Son J-D, Yang B-S, Tan ACC, Gu D-S, et al. Fault Diagnosis of Low Speed Bearing based on Relevance Vector Machine and Support Vector Machine. *Expert Syst Appl.* 2009 Apr;36(3, Part 2):7252–7261.

33. Rai VK, Mohanty AR. Bearing Fault Diagnosis using FFT of Intrinsic Mode Functions in Hilbert–Huang Transform. *Mech Syst Signal Process.* 2007 Aug;21(6):2607–2615.

34. Wang CC, Kang Y, Liao CC. Using Bayesian Networks in Gear Fault Diagnosis. *Appl Mech Mater.* 2013 Jan;284-287:2416–2420.

35. Mao Z, Todd M. Statistical Modeling of Frequency Response Function Estimation for Uncertainty Quantification. *Mech Syst Signal Process.* 2013 Jul 20;38(2):333–345.

36. Mao Z, Todd M. A model for quantifying uncertainty in the estimation of noise-contaminated measurements of transmissibility. *Mech Syst Signal Process.* 2012 Apr;28:470–481.

37. Welch P. The Use of Fast Fourier Transform for the Estimation of Power Spectra: A Method Based on Time Averaging Over Short, Modified Periodograms. *IEEE Trans Audio Electroacoustics.* 1967;15:70–73.